Structure and Dynamic Properties of Solid L-Tyrosine-Ethylester as Seen by ^{13}C MAS NMR

Xavier Helluy and Angelika Sebald*

Bayerisches Geoinstitut, Universität Bayreuth, 95440 Bayreuth, Germany

Received: December 14, 2002; In Final Form: February 11, 2003

^{13}C MAS NMR experiments on solid L-tyrosine-ethylester with ^{13}C in low natural abundance and in fully ^{13}C enriched form are reported. The phenyl rings are found to undergo π flips with a rather low activation energy $E_a = 50 \pm 12$ kJ mol^{-1}. In addition, the ester groups are afflicted by dynamic disorder at all temperatures accessible to MAS NMR experiments. Zero-quantum homonuclear ^{13}C recoupling experiments on fully ^{13}C enriched L-tyrosine-ethylester were carried out at low temperature. These experiments faithfully reproduce those molecular structural features, known from single-crystal X-ray diffraction, that are defined by short-range $^{13}C-^{13}C$ interactions but fail to uniquely characterize the complete molecular conformation defined by intermediate-range $^{13}C-^{13}C$ interactions.

Introduction

Solid-state magic-angle-spinning (MAS) NMR experiments generating quantitative structural information, for example by characterizing internuclear distance connectivities via measurements of dipolar coupling constants, are important in terms of methodology development as well as increasingly in terms of applications. Numerous so-called recoupling experiments for homo- and heteronuclear spin systems under MAS conditions[1,2] have been developed in the past years, in particular for spin-$^1/_2$ systems. Many such experiments lend themselves to in-depth quantitative analysis by means of numerically exact simulations as long as one is dealing with spatially isolated (re)coupled spin systems of limited size. In practice, however, we are often faced with extended spin systems. For example, these could be ^{31}P spin systems in condensed inorganic phosphates or, similarly, ^{13}C spin systems in fully ^{13}C enriched (bio)organic solids. Especially for fully ^{13}C-enriched (bio)organic solids, recently promising experimental protocols have been reported which demonstrate that in favorable cases enough geometric constraints may be obtained from dipolar recoupling experiments in order to permit the reconstruction of the three-dimensional solid-state structure of an organic molecule,[3−5] in spirits not unsimilar to established procedures in solution-state NMR of bioorganic compounds.

Here we will take an opposite approach in that we will consider ^{13}C MAS NMR experiments on an organic solid with known crystal structure. We will investigate the structural and dynamic properties of solid L-tyrosine-ethylester with ^{13}C in natural abundance (TEE) as well as in its fully ^{13}C enriched form (U^{13}C-TEE). The structure of TEE has been determined by single-crystal X-ray diffraction at room temperature.[6] TEE in a pairwise selectively ^{13}C-labeled version had previously been used to demonstrate measurements of internuclear $^{13}C-^{13}C$ distances by means of rotational-resonance based ^{13}C MAS experiments,[7,8] whereas U^{13}C-TEE had been used to probe the selectivity of ^{13}C rotational-resonance double-quantum filtered experiments on multi-^{13}C spin systems.[9] Here we will focus on the question what we may have learnt about the three-dimensional molecular structure of TEE if the crystal structure would not be known, and which precautions need to be taken in order to obtain reliable structural information from MAS NMR experiments.

Experimental Section

Sample. L-Tyrosine-ethylester with ^{13}C in natural abundance (TEE) is commercially available (Aldrich Chemicals). The synthesis and single-crystal X-ray diffraction structure of TEE are described in the literature.[6] Our sample of fully ^{13}C enriched L-tyrosine-ethylester (U^{13}C-TEE) was provided by C. Griesinger and C. Hoffmann, Göttingen. The purity and identity of both samples were checked by solution-state NMR and powder X-ray diffraction.

NMR Experiments. Variable-temperature one-dimensional ^{13}C MAS NMR experiments and two-dimensional (2D) MAS exchange experiments (EXSY)[10] on TEE, as well as rotational-resonance double-quantum filtration experiments[9,11] on U^{13}C-TEE were carried out using Bruker MSL 200 and MSL 300 NMR spectrometers. The corresponding ^{13}C Larmor frequencies are $\omega_0/2\pi = -50.3$ MHz and $\omega_0/2\pi = -75.4$ MHz, respectively. ^{13}C RIL [12] experiments on U^{13}C-TEE were carried out at $T = 240$ K, using a Bruker DMX 300 NMR spectrometer ($\omega_0/2\pi = -75.4$ MHz). Standard 4 mm double-bearing Bruker CP MAS probes were used. Approximately 15 mg of U^{13}C-TEE were packed in the center part of the rotor in an insert (Kel-F) with a spherical cavity. MAS frequencies $\omega_r/2\pi$ were generally in the range 2−8 kHz and were actively controlled to within ±2 Hz. All ^{13}C MAS spectra were obtained with $^1H \rightarrow {}^{13}C$ cross polarization (CP) with contact times of 2 ms and recycle delays of 2 s. ^1H and ^{13}C $\pi/2$ pulse durations were in the range 2.5−4.0 μs. For ^{13}C RIL experiments on U^{13}C-TEE at $T = 240$ K, the MAS frequency was $\omega_r/2\pi = 8$ kHz, TPPM ^1H decoupling[13] was applied during acqusition, 8 transients per t_1 increment and 512 spectra per experiment were accumulated in the 2D data sets; 19 2D experiments with mixing times τ_{mix} ranging from $\tau_{mix} = 0.6$ ms to $\tau_{mix} = 25$ ms were recorded.

Definitions and Simulations. Shielding notation is used, and the signs of frequencies have been defined elsewhere.[14] Isotropic ^{13}C shielding values are given relative to the ^{13}C resonance of external $SiMe_4$ at 0 ppm. All numerical simulations were carried

* To whom correspondence should be addressed. E-mail: angelika.sebald@uni-bayreuth.de.

10.1021/jp0277210 CCC: $25.00
Published on Web 03/15/2003

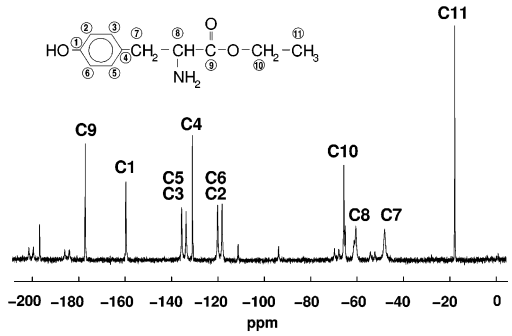

Figure 1. ^{13}C MAS NMR spectrum of TEE at $T = 250$ K ($\omega_0/2\pi = -75.4$ MHz, $\omega_r/2\pi = 4970$ Hz; all nonlabeled resonances are spinning sidebands); also given is the assignment (see below, Figure 3). The numbering scheme is identical with the scheme used in the description of the single-crystal X-ray diffraction structure of TEE.[6]

out using the MATLAB package.[15] A full description of the analysis procedures of RIL experiments within the exchange matrix formalism, with the spin diffusion exchange rate constants being proportional to the square of the corresponding dipolar coupling constant and thus inversely proportional to the sixth power of the internuclear distance, is given elsewhere.[16,17]

Results and Discussion

In the following, we will first consider variable-temperature ^{13}C MAS NMR experiments on TEE. The second section deals with low-temperature ^{13}C MAS NMR spin-diffusion experiments on fully ^{13}C enriched L-tyrosine-ethylester, U^{13}C-TEE. In the final section, we will discuss some of the implications and issues raised by the experimental NMR results obtained on solid L-tyrosine-ethylester.

Variable Temperature ^{13}C MAS NMR of TEE. A ^{13}C MAS NMR spectrum of TEE at $T = 250$ K is depicted in Figure 1. In agreement with the predictions of the single-crystal X-ray diffraction structure of TEE,[6] each of the 11 carbon sites in the molecule gives rise to a ^{13}C resonance, and all eleven resonances are resolved. This statement is only true for ^{13}C MAS NMR spectra of TEE taken at low temperatures. Upon raising the temperature, spectral changes in the region of the aromatic ^{13}C resonances occur. This is shown in Figure 2. The pairs of ^{13}C5,^{13}C3 and ^{13}C6,^{13}C2 resonances gradually broaden and pairwise merge at temperatures exceeding 310 K. The origin of this effect lies in the molecular dynamic solid-state properties of TEE. Mutual chemical exchange of the aromatic carbon sites C5−C3 and C6−C2 by π flips of the phenyl ring around its C1−C4 axis is proven by 2D EXSY experiments at $T = 290$ K. The π flips of the phenyl ring lead to exchange broadening and coalescence in the ^{13}C MAS NMR spectra in the temperature range $T = 270-340$ K (see Figure 2). The exchange rate constants (see Figure 2) of the process are obtained from line shape simulations of the variable-temperature ^{13}C MAS NMR spectra. An Arrhenius plot of the exchange rate constants as a function of temperature yields an activation energy $E_a = 50 \pm 12$ kJ mol^{-1} for the π flips of the phenyl ring in solid TEE (see the Supporting Information for details). π Flips of phenyl rings in solid organic aromatic compounds occur quite commonly. For several aromatic compounds, these solid-state dynamics previously have been investigated by solid-state NMR techniques.[18−26] The literature data demonstrate a large variation of the activation energy of phenyl π flips in organic solids, ranging from ca. 51 kJ mol^{-1} in a penicillin salt to ca. 111 kJ mol^{-1} in another pencillin derivative[20] and many other examples such as para-iodo-benzene, biphenyl, or other compounds[18−26] displaying activation energies between these two extremes. The activation energy of the π flips of the phenyl ring in solid TEE is thus one of the lowest activation barriers for this kind of dynamic disorder in organic solids observed so far.

Inspection of the crystal structure of TEE (see below, Figure 4) offers an immediate explanation for the relatively low activation barrier of the π flips of the phenyl ring. The preliminary variable temperature ^{13}C MAS NMR experiments on TEE further define the temperature range for meaningful experiments aiming to determine structural parameters such as

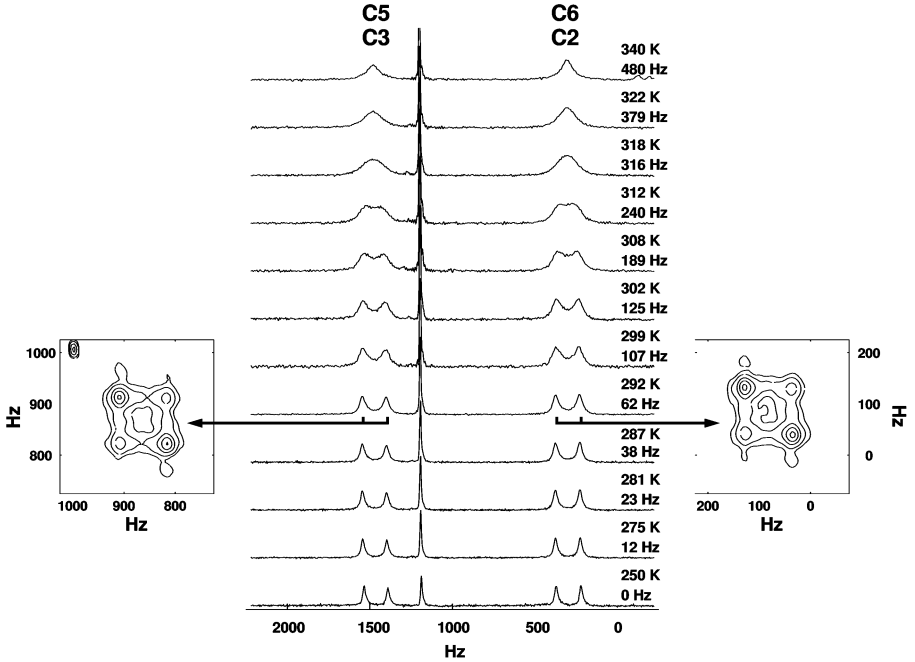

Figure 2. Variable-temperature ^{13}C MAS NMR spectra of TEE ($\omega_0/2\pi = -75.4$ MHz, $\omega_r/2\pi = 4970$ Hz), only the region of the aromatic ^{13}C resonances is shown. Temperatures and corresponding exchange rate constants (derived from line shape simulations, data not shown) of the π flip of the phenyl ring are indicated. Also shown are the respective ^{13}C3,^{13}C5 and ^{13}C2,^{13}C6 regions of contour plots of a ^{13}C 2D EXSY experiment at $T = 290$ K ($\omega_0/2\pi = -50.3$ MHz, $\omega_r/2\pi = 5000$ Hz, $\tau_{mix} = 7.5$ ms), demonstrating the exchange in the C3,C5 and C2,C6 pairs of sites.

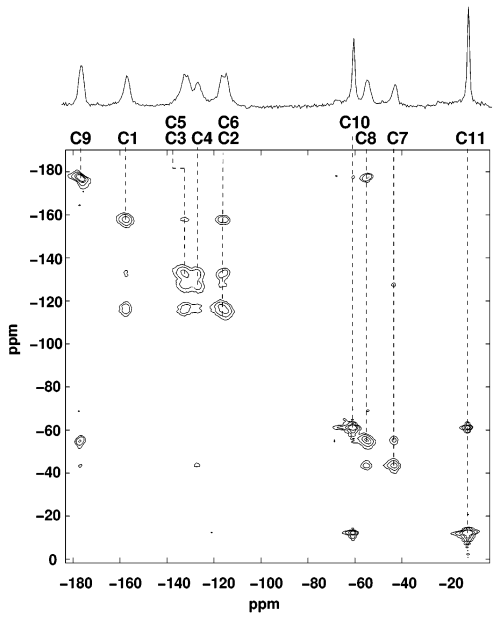

Figure 3. Contour plot of a ^{13}C RIL [12] experiment with short mixing time ($\tau_{mix} = 1.87$ ms, $\omega_0/2\pi = -75.4$ MHz, $\omega_r/2\pi = 8000$ Hz) on U^{13}C-TEE at $T = 240$ K, highlighting the short-range connectivities and providing spectral assignment as indicated (see also Figure 1). Also shown is the projection of the corresponding one-dimensional ^{13}C MAS NMR spectrum of U^{13}C-TEE.

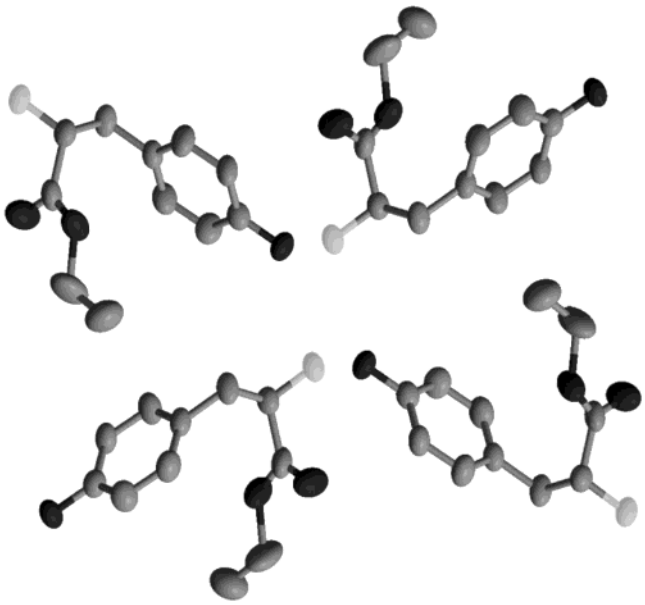

Figure 4. Perspective view of the molecular and crystal structure of TEE at room-temperature according to single-crystal X-ray diffraction.[6]

internuclear distances from homonuclear dipolar recoupling ^{13}C MAS NMR experiments on U^{13}C-TEE: the temperature must be chosen low enough to ensure that the flip rate of the phenyl ring is small enough in order not to interfer with any internuclear distance-determination experiments. For U^{13}C-TEE, this requires working at temperatures $T < 260$ K.

Low Temperature ^{13}C RIL Experiments on ^{13}C-Labeled L-Tyrosine-ethylester U^{13}C-TEE. An isolated molecule of U^{13}C-TEE represents a cluster of eleven dipolar coupled ^{13}C spins, arranged in a specific topology. Suppose the spectral assignment is known and all internuclear $^{13}C-^{13}C$ distances in this cluster were known. This information would be equivalent with knowing the molecular structure because enough so-called through-space connectivities would exist as constraints for defining the geometry of the molecule. Of the many existing experimental options to carry out homonuclear dipolar recoupling experiments[1,2] aiming to generate such geometrical constraints via the measurement of dipolar coupling constants, here we chose the RIL experiment[12] in its zero-quantum spin-dynamics version. Exploitation of the zero-quantum spin dynamics (spin diffusion) as opposed to experiments exploiting double-quantum spin dynamics may be advantageous when dealing with attempts to quantify internuclear distances in multispin systems. In addition, it was previously shown on several condensed inorganic phosphate phases[16,17] that so-called spin-diffusion build-up curves obtained from a series of RIL experiments with different mixing times faithfully reproduce build-up curves calculated from the corresponding crystal structures. The data analysis follows an exchange-matrix formalism[10] and basically assumes an ideal performance of the RIL experiment, i.e., it assumes the generation of a purely "dipolar Hamiltonian", neglecting chemical shielding anisotropies and homonuclear *J*-coupling interactions. Ensuring the validity of the assumption of dealing with a purely "dipolar Hamiltonian" necessitates a careful choice of the experimental conditions. To avoid unwanted influences from chemical shielding anisotropies, it is prudent to run these experiments at the lowest reasonable Larmor frequency where full spectral resolution is obtained without having to resort to unreasonably high MAS frequencies. Very high MAS frequencies are undesirable for reasons of rf limitations and generally are not the regime of optimum performance of RIL expertiments.[27] In addition, optimum ^1H-decoupling performance is essential in isolating the ^{13}C spins from the surrounding numerous ^1H spins in the lattice.

With these considerations and with the dynamic disorder of the phenyl ring in mind, our ^{13}C RIL experiments on U^{13}C-TEE were carried out at $T = 240$ K, at a ^{13}C Larmor frequency $\omega_0/2\pi = -75.4$ MHz and using a MAS frequency $\omega_r/2\pi = 8$ kHz. Figure 3 shows the contour plot of a ^{13}C RIL experiment with a mixing time short enough ($\tau_{mix} = 1.87$ ms) to solely depict the shortest internuclear $^{13}C-^{13}C$ distances (directly bonded carbon atoms), thus in a first step providing assignment of the eleven ^{13}C resonances to carbon sites C1 to C11. Numerous alternative experimental options for assignment strategies in homonuclear multispin systems exist, often based on *J*-coupling connectivities rather than on dipolar coupling networks. RIL experiments with short mixing times are only one of many possibilities. For more complicated larger spin systems, *J*-coupling based assignment strategies may sometimes offer more straightforward results. The strengths of RIL experiments usually come into play after the assignment is made.[17] The eleven-spin system in U^{13}C-TEE is simple enough so that straightforward inspection of a single RIL experiment with short mixing time permits assignment (see Table 1). Only the assignment within the C3,C5 and C2,C6 pairs of sites remains undetermined form this experiment. Two assignment permutations are possible, either $^{13}C5-^{13}C3$ and $^{13}C2-^{13}C6$ or $^{13}C3-^{13}C5$ and $^{13}C6-^{13}C2$ (in the order of increasing shielding of the four ^{13}C resonances).

Figure 4 depicts the three-dimensional structure of the TEE molecule as well as the packing of the molecules in the crystal lattice. The most important features of the structure are the following. The ester tail is slightly bent back toward the plane of the phenyl ring ("scorpion-like"), leading to relatively short distances between the carbon atoms of the phenyl ring and those in the ethyl group. Note that the carbon atoms of the ethyl group are only fairly poorly defined from the single-crystal X-ray

TABLE 1: Isotropic ^{13}C Chemical Shielding Values [ppm] and Assignment for Solid L-tyrosine-ethylester

carbon site	1	2,6	3,5	4	7	8	9	10	11
ω^{CS}_{iso}	−156.3	−116.8; −115.0	−132.2; −130.8	−127.9	−44.9	−56.8	−174.1	−62.4	−14.6

TABLE 2: Intra- and Intermolecular Distances [pm] between the Methyl−Carbon Site C11 and the Phenyl Ring Carbon Sites C1 to C6 in Solid L-Tyrosine-ethylester[6]

distances [pm]	C11−C1	C11−C2	C11−C3	C11−C4	C11−C5	C11−C6
intramolecular	477	490	482	469	457	464
intermolecular	451	386	368	366	380	415

diffraction study, displaying large thermal displacement ellipsoids at ambient temperature.[6] The packing of the TEE molecules is such that short contacts via hydrogen bonding between the phenolic OH group and the NH_2 group of the neighboring molecule result in zigzag-like chains of molecules where additional contacts are induced between the ester group of a TEE molecule in one chain and the phenyl ring of the nearest TEE molecule in the adjacent chain. In fact, the *intra*molecular distances between the methyl carbon atom C11 and the carbon sites C1 to C6 are longer than the *inter*molecular distances of this methyl carbon atom C11 to all carbon sites C1 to C6 of the phenyl ring in the nearest neighbor molecule (see Table 2). Figure 4 further illustrates and explains the low activation barrier of the π flip of the phenylring: the crystal packing leaves room for these reorientational jumps of the phenyl ring. Even more pronounced is the amount of space which the crystal packing leaves for the ester groups to occupy. They sit in hollow cages without their direct surroundings strongly enforcing a particular conformation for reasons of steric congestion. This points toward some dynamic disorder of the ester groups and is in agreement with the large thermal displacement parameters found by single-crystal X-ray diffraction at ambient temperature.

The Cartesian coordinates of all carbon sites as determined by X-ray diffraction are easily converted into a data matrix describing the three-dimensional arrangement of the atoms by a set of multiple internuclear distances. After converting the distances into a set of dipolar coupling constants, a set of predicted ^{13}C RIL spin-diffusion build-up curves based on the crystal structure is easily calculated within the exchange matrix formalism. [10] One can do this by taking only an isolated molecule into account, or by including as many additional atoms/^{13}C spins in the vicinity as is necessary, depending on the crystal structure. This is illustrated in Figure 5 where calculated build-up curves for an isolated TEE molecule (in blue) are shown in comparison with build-up curves based on all interacting spins within a radius of 550 pm around each site (in red). The multiple intermolecular contacts in solid U^{13}C-TEE lead to only small differences between calculated spin-diffusion build-up curves based on an isolated molecule and those including nearby molecules/^{13}C spins; mainly the low-amplitude build-up curves relating the carbon atoms C10 and C11 of the ethyl group with the carbon atoms of the phenyl rings would be systematically slightly underestimated by considering an isolated molecule. We find that a radius of 550 pm represents a reasonable cutoff distance in providing a realistic picture of the ^{13}C spin diffusion build-up curves in solid U^{13}C-TEE.

The isolated versus nonisolated molecule scenario depicted in Figure 5 mainly rests on differences in the number of intermediate-range internuclear distances in the 400−500 pm range contributing to the individual build-up curves but resulting in only small differences in the overall behavior. Also the orientation of the ester group relative to the phenyl ring in an

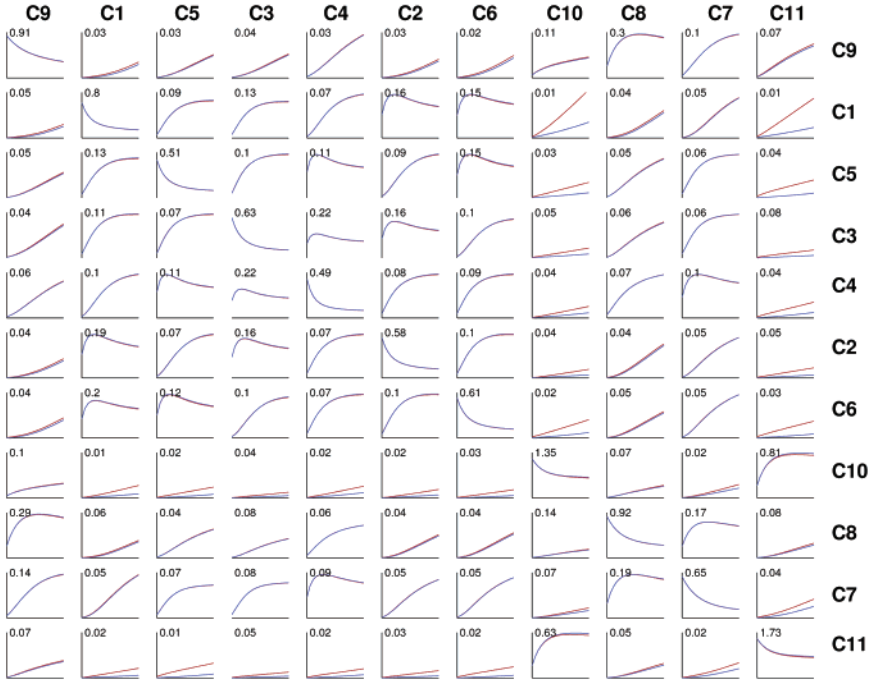

Figure 5. ^{13}C spin-diffusion build-up curves, calculated from the X-ray diffraction structure of L-tyrosine-ethylester. The curves are arranged matrix-like in the order of the ^{13}C NMR spectra as indicated for one of the two possible assignment permutations (see text). The red curves take into account all carbon atoms within a 550 pm radius, and the blue curves are calculated for an isolated molecule. The *x* axes in the plots are time scales, running from 0 to 25 ms; the *y* axes represent peak intensities in arbitrary units as indicated in the figure for each curve. Note that the scales of the *y* axes vary by 2 orders of magnitude. The inherent asymmetries of some related build-up curves $^{13}C(n) \rightarrow {}^{13}C(m)$ versus $^{13}C(m) \rightarrow {}^{13}C(n)$ result from the unequal intensities of the 11 ^{13}C resonances in experimental spectra of U^{13}C-TEE from cross polarization and are already taken into account here (compare Figures 1 and 3).

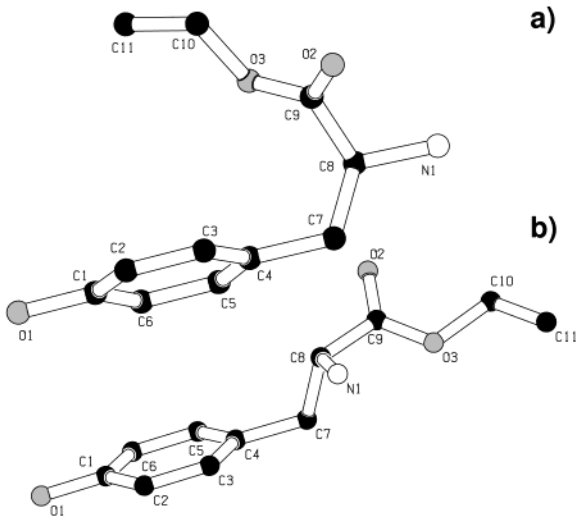

Figure 6. Two strongly differing molecular conformations of TEE. (a) The molecular conformation as determined by single-crystal X-ray diffraction. (b) A grossly different orientation of the ester tail relative to the phenyl ring.

isolated TEE molecule is described by a set of intermediate-range internuclear distances in the 400−500 pm range between the aliphatic and the aromatic carbon atoms. For example, we find that even drastic changes in the orientation of the ester group relative to the phenyl ring (see Figure 6) would not result in significant and traceable changes in the corresponding predicted set of build-up curves (calculated for an isolated molecule; data not shown). It appears that, for structure-determination tasks in this range of internuclear distances, ^{13}C NMR experiments on strategically selectively ^{13}C enriched samples are the more promising approach.

The spin diffusion build-up curves depicted in Figure 7 summarize how a series of 19 ^{13}C RIL experiments with mixing times in the range 0.6−25 ms characterize the structure of U^{13}C-TEE. The red lines are the build-up curves as calculated from the X-ray diffraction structure and take into account all atoms within a 550 pm radius. The gray dots are the experimentally determined normalized integrated intensities of all ^{13}C peaks, plotted as a function of the RIL mixing times. The overall agreement between predicted and observed build-up curves is reasonable, especially so because the amplitudes of the various different cross-peak build-up curves from (multiple) short, intermediate, and long distances vary by 2 orders of magnitude. These general features are well reproduced in the ^{13}C RIL experiments. The two possible assignment permutations for the ^{13}C3,^{13}C5 and ^{13}C2,^{13}C6 pairs remain indistinguishable.

Several points are noticeable where the agreement between predicted and observed build-up curves is less than perfect. The small-amplitude build-up curves relating, for example, ^{13}C5 and ^{13}C3 or ^{13}C6 and ^{13}C2, are afflicted by a certain lack of spectral resolution at our experimental conditions, leading to fairly large relative integration errors and scatter of the experimental data points. Large differences in line widths (for instance, ^{13}C8 versus ^{13}C11) furthermore lead to differing accuracies in integrating the respective peak areas. The experimental build-up curves connecting ^{13}C9 and ^{13}C10 are significantly higher than the predicted build-up curves. This is likely to be due to the fact that these two ^{13}C resonances are close to the $n = 1$ rotational-resonance (R^2) condition (within 500 Hz) at a MAS frequency $\omega_r/2\pi = 8000$ Hz. Similar systematically overestimated build-up behavior in RIL experiments we have previously observed for ^{31}P spins close to the $n = 0$ R^2 condition.[17]

The most striking systematic disagreement, however, is observed for the build-up behavior of the intense cross-peaks connecting ^{13}C10 and ^{13}C11 in the ethyl group. According to the single-crystal X-ray diffraction study, the internuclear distance between these two carbon atoms should be very short (138 pm, corresponding to a dipolar coupling constant of −2858 Hz),[6] whereas the ^{13}C RIL results suggest a much smaller dipolar coupling constant between ^{13}C10 and ^{13}C11. This finding is in

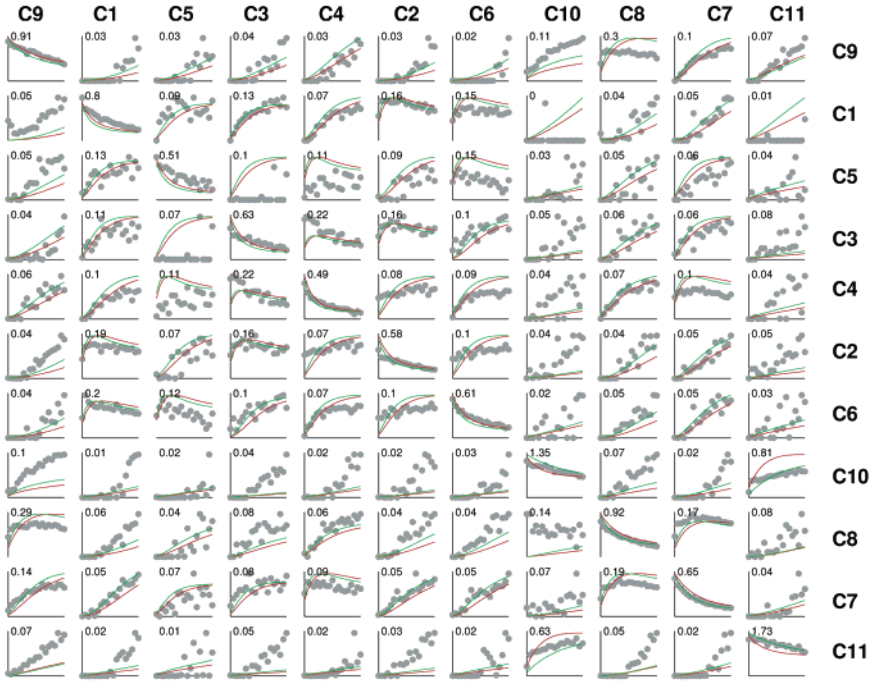

Figure 7. Experimental ^{13}C spin-diffusion build-up curves for U^{13}C-TEE at $T = 240$ K (grey dots) in comparison with the build-up curves calculated for a nonisolated molecule (red curves). The arrangement of the build-up curves and scales of the x and y axes in the individual plots are the same as in Figure 5. The green curves are calculated by taking the ^{13}C10−^{13}C11 dipolar coupling constant as −1400 Hz (see text) and yield improved overall agreement with the experimental data. Note that the scales of the y axes vary by 2 orders of magnitude.

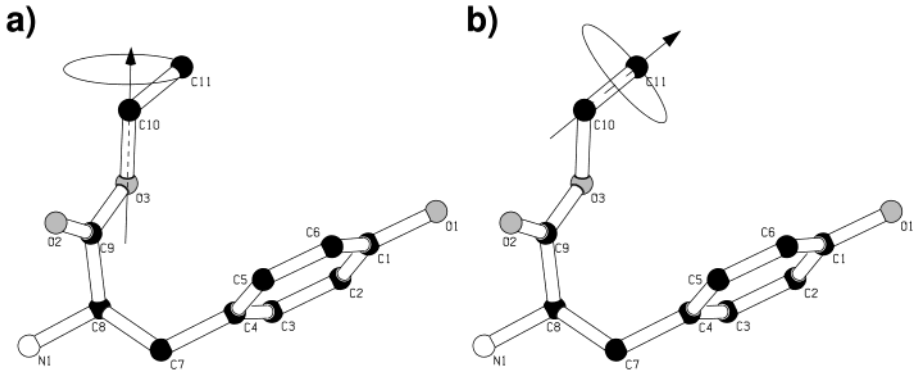

Figure 8. Two models of dynamic disorder affecting the ester tail in solid L-tyrosine-ethylester. (a) Rotation of the $^{13}C10-^{13}C11$ bond vector around the O3-$^{13}C10$ bond direction. (b) Nutation of the $^{13}C10-^{13}C11$ bond vector around its mean direction.

full agreement with our earlier results from ^{13}C rotational-resonance double-quantum filtration (R^2-DQF) experiments focused on the $^{13}C10$,$^{13}C11$ pair in U^{13}C-TEE.[9] These earlier R^2-DQF experiments on U^{13}C-TEE at room temperature yielded line shapes corresponding to an apparent dipolar coupling constant of only -1400 Hz between $^{13}C10$ and $^{13}C11$. This, however, would correspond to an unreasonably long one-bond distance of 175 pm. Repeating these ^{13}C R^2-DQF experiments at $T = 170$ K (data not shown) yields line shapes identical to those observed at room temperature and thus correspond to the same apparent, small dipolar coupling constant of only -1400 Hz. Obviously, apart from the slow π flips of the phenyl ring, solid L-tyrosine-ethylester features yet another dynamic disorder property leading to a partial averaging of the dipolar coupling interaction between $^{13}C10$ and $^{13}C11$. If we were faced with another slow process of the chemical-exchange type on the kHz time scale, it would have to have a very low activation barrier if no difference in the ^{13}C R^2-DQF line shapes is found over a temperature range of 120°. It is more likely that the ethyl group is not affected by some such discrete jump processes but by a more random and much faster, diffusive type of disorder affecting mainly the location of the methyl carbon atom. This would also be in agreement with the large thermal displacement ellipsoid found by X-ray diffraction for this atom (and, in fact also for C10; see Figure 4). It remains to rationalize these findings in terms of a reasonable disorder model, two possible such disorder models are illustrated in Figure 7. If one takes the C10−C11 bond distance as 138 pm from the unrefined X-ray diffraction value[6] (corresponding to a $^{13}C10-^{13}C11$ dipolar coupling constant of -2858 Hz) and assumes rotation of the C10−C11 bond vector in the fast motion limit[28] around the direction of the adjacent O3−C10 bond axis (see Figure 8a)), this would result in a partially averaged $^{13}C10-^{13}C11$ dipolar coupling constant of -927 Hz, considerably less than the value of -1400 Hz which we find experimentally. Of course, the deviation is even larger when assuming the same type of motion but a more realistic C10−C11 bond distance of 155 pm, here the static value of the $^{13}C10-^{13}C11$ dipolar coupling constant would amount to -2050 Hz and would be motionally averaged to -674 Hz in the fast motion limit. A perhaps more realistic disorder model could be a rapid nutation of the C10−C11 bond vector around its main direction (see Figure 8 b). If such a dynamic disorder process would occur rapidly with a cone angle of 25−30°, this would result in a partially averaged $^{13}C10-^{13}C11$ dipolar coupling constant of ca. -1400 Hz, in agreement with the experimentally estimated value. It is not possible to positively proof this particular disorder model; in reality, it is probably more complicated than a nutation-disorder model involving just one axis: as one can see from the X-ray diffraction data, also C10 displays a large thermal displacement ellipsoid. Nevertheless, physically meaningful disorder models capable of reproducing the experimental NMR results can be found. Clarification of the precise nature of the dynamic disorder of the aliphatic ester side chain in solid L-tyrosine-ethylester was not attempted in the original single-crystal-X-ray diffraction study[6] and would require additional extended variable-temperature diffraction and/or molecular modeling studies. Finally, returning briefly to the build-up curves in Figure 7, it is easily seen that calculated build-up curves based on an apparent dipolar coupling constant of -1400 Hz between $^{13}C10$ and $^{13}C11$ (green curves) agree better with the experimentally observed data than do the calculated build-up curves (red curves) not taking the partial averaging of this dipolar coupling interaction into account.

Some General Considerations. Because of its structural and dynamic solid-state properties L-tyrosine-ethylester should not be used anymore as a model compound for testing dipolar recoupling experiments. However, L-tyrosine-ethylester is by no means an exotic organic solid. In that regard, the ^{13}C MAS NMR experiments reported here emphasize the importance of dynamic solid-state properties when aiming at structure-determination of organic solids by means of dipolar recoupling NMR experiments in a more general context. Whereas dynamic processes such as π flips of phenyl rings may be sufficiently slowed by sample cooling, other dynamic disorder properties, such as the disorder of the ester tail observerd for TEE, cannot be frozen out. In the absence of such molecular dynamic effects, recent NMR work on solid peptides where the molecular backbone represents a rigid moiety have demonstrated the power of structure-determination strategies based on solid-state NMR data alone.[29,30] In contrast, obviously dynamic solid-state properties leading to partial averaging of dipolar coupling interactions may be a source of severe errors in structure-determination NMR experiments where present and if not taken into account. Similar disorder effects as observed here for solid TEE are likely to occur, for instance, in aliphatic side chains of many organic solids. Accordingly, structural parameters extracted from the corresponding ^{13}C spectral regions should be cautiously interpreted. The results of our ^{13}C RIL experiments on U^{13}C-TEE further illustrate that structural constraints from short internuclear distances are obtained in a rather robust manner. However, structural refinement depending on intermediate internuclear distances may not be possible entirely from experiments on fully ^{13}C labeled samples alone, at least not when relying solely on broadbanded dipolar recoupling NMR experiments. Structural refinement, in particular concerning questions about molecular conformations, may thus require additional experiments on additional, selectively labeled samples (where

possible) and/or additional NMR experiments with a highly narrowbanded profile (i.e., selective schemes) on the fully labeled sample.

Acknowledgment. Financial support of this work by the Deutsche Forschungsgemeinschaft is gratefully acknowledged. We thank C. Griesinger and C. Hoffmann, Göttingen, for their generous donation of our sample of U^{13}C-TEE. We are grateful to A. Kentgens and the entire group at the Department of Physical Chemistry/Solid State NMR, University of Nijmegen, The Netherlands, for their hospitality and for giving us access to their DMX 300 NMR spectrometer. We thank S. Dusold and J. Kümmerlen for their cooperation at some early stages of this work.

Supporting Information Available: (i) Arrhenius plot of all exchange rate constants of the π flip in solid TEE from variable-temperature one-dimensional ^{13}C MAS NMR; (ii) plot comparing experimental and best-fit simulated variable-temperature ^{13}C MAS NMR spectra of TEE. This material is available free of charge via the Internet at http://pubs.acs.org.

References and Notes

(1) Bennett, A. E.; Griffin, R. G.; Vega, S. Recoupling of homo- and heteronuclear dipolar interactions in rotating solids. In *Solid-State NMR IV: Methods and Applications of Solid-State NMR; Vol. 33 NMR Basic Principles and Progress*; Blümich, B., Ed.; Springer-Verlag: Berlin, 1994; pp 1−78.

(2) Dusold, S.; Sebald, A. Dipolar recoupling under magic-angle-spinning conditions. In *Annual Reports on NMR Spectroscopy*; Webb, G., Ed.; Academic Press: London, 2000; Vol. 41, pp 185−264.

(3) Jaroniec, C. P.; Tounge, B. A.; Herzfeld, J.; Griffin, R. G. *J. Am. Chem. Soc.* **2001**, *123*, 3507.

(4) Jaroniec, C. P.; Filip, C.; Griffin, R. G. *J. Am. Chem. Soc.* **2002**, *124*, 10728.

(5) Rienstra, C. M.; Hohwy, M.; Mueller, L. J.; Jaroniec, C. P.; Reif, B.; Griffin, R. G. *J. Am. Chem. Soc.* **2002**, *124*, 11908.

(6) Pieret, A. F.; Durant, F.; Griffé, M.; Germain, G.; Debaerdemaeker, T. *Acta Crystallogr. B* **1970**, *26*, 2117.

(7) Raleigh, D. P.; Creuzet, F.; Das Gupta, S. K.; Levitt, M. H.; Griffin, R. G. *J. Am. Chem. Soc.* **1989**, *111*, 4502.

(8) Costa, R. R.; Sun, B.; Griffin, R. G. *J. Am. Chem. Soc.* **1997**, *119*, 10821.

(9) Dusold, S.; Sebald, A. *J. Magn. Reson.* **2000**, *145*, 340.

(10) Ernst, R. R.; Bodenhausen, G.; Wokaun, A. *Principles of Nuclear Magnetic Resonance in One and Two Dimensions*; Clarendon Press: Oxford, 1987.

(11) Karlsson, T.; Edén, M.; Luthman, H.; Levitt, M. H. *J. Magn. Reson.* **2000**, *145*, 340.

(12) Baldus, M.; Meier, B. H. *J. Magn. Reson.* **1997**, *128*, 172.

(13) Bennett, A. E.; Rienstra, C. M.; Auger, M.; Lakshmi, K. V.; Griffin, R. G. *J. Chem. Phys.* **1995**, *103*, 6951.

(14) Levitt, M. H. *J. Magn. Reson.* **1997**, *126*, 164.

(15) MATLAB, version 6.5; The Mathworks Inc.: Natick, MA, 2002.

(16) Dusold, S.; Kümmerlen, J.; Schaller, T.; Sebald, A. Dollase, W. A. *J. Phys. Chem. B* **1997**, *101*, 6359.

(17) Helluy, X.; Marichal, C. Sebald A. *J. Phys. Chem. B* **2000**, *104*, 2836.

(18) Reichert, D.; Zimmermann, H.; Tekel, P.; Poupko, R.; Luz, Z. *J. Magn. Reson.* **1997**, *125*, 245.

(19) Reichert, D.; Hempel, G.; Zimmermann, H.; Schneider, H.; Luz, Z. *Solid State Nucl. Magn. Reson.* **2000**, *18*, 17.

(20) Wendeler, M.; Fattah, J.; Twyman, J. M.; Edwards, A. J.; Dobson, C. M.; Heyes, S. J.; Prout, K. *J. Am. Chem. Soc.* **1997**, *119*, 9793.

(21) Riddell, F. G.; Bremner, M.; Strange, J. H. *Magn. Reson. Chem.* **1994**, *32*, 118.

(22) Aliev, A. E.; Harris, K. D. M.; Alcobé, X.; Estop, E. *J. Chem. Soc. Faraday Trans.* **1993**, *89*, 3797.

(23) Stumber, M.; Zimmermann, H.; Schmitt, H.; Haeberlen, U. *Mol. Phys.* **2001**, *99*, 1091.

(24) Bräuniger, T.; Poupko, R.; Luz, Z.; Reichert, D.; Zimmermann, H.; Schmitt, H.; Haeberlen, U. *Phys. Chem. Chem. Phys.* **2001**, *3*, 1891.

(25) Müller, A.; Haeberlen, U. *Chem. Phys. Lett.* **1996**, *248*, 249.

(26) Speier, P.; Müller, A.; Meinel, C.; Haeberlen, U. *Mol. Phys.* **1998**, *95*, 859.

(27) Brinkmann, A.; Schmedt auf der Günne, J.; Levitt, M. H. *J. Magn. Reson.* **2002**, *156*, 79.

(28) Schmidt-Rohr, K.; Spiess, H. W. *Multidimensional Solid-State NMR and Polymers*; Academic Press: London, 1994.

(29) Rienstra, C. M.; Tucker-Kellogg, L.; Jaroniec, C. P.; Hohwy, M.; Reif, B.; McMahon, M. T.; Tidor, B.; Lozano-Pérez, T.; Griffin, R. G. *Proc. Natl. Acad. Sci. U.S.A.* **2002**, *99*, 10260.

(30) Jaroniec, C. P.; MacPhee, C. E.; Astrof, N. S.; Dobson, C. M.; Griffin, R. G. *Proc. Natl. Acad. Sci. U.S.A.* **2002**, *99*, 16748.